SERBIAN JOURNAL OF ELECTRICAL ENGINEERING
Vol. 11, No. 4 (special issue), December 2014, 565-584

UDC: 621.372.543:681.515 **DOI: 10.2298/SJEE1404565S**

Active RC Filter Based Implementation Analysis Part of Two Channel Hybrid Filter Bank

Vidosav Stojanović[1], Negovan Stamenković[2], Nikola Stojanović[1]

Abstract: In the present paper, a new design method for continuous-time power-symmetric active RC filters for Hybrid Filter Bank (HFB) is proposed. Some theoretical properties of continious-time power-symmetric filters bank in a more general perspective are studied. This includes the derivation of a new general analytical form, and a study of poles and zeros locations in *s*-plane. In the proposed design method the analytic solution of filter coefficients is solved in *s*-domain using only one nonlinear equation Finally, the proposed approximation is compared to standard approximations. It was shown that attenuation and group delay characteristic of the proposed filter lie between Butterworth and elliptic characteristics.

Keywords: Hybrid filter bank, Continuous-time filters, Allpass network, Active RC filter.

1 Introduction

Many continuous-time signals have a low level in nature, such as the output of sensors, moreover hybrid filter bank have been often used for time-frequency decomposition, processing, recognition, and storage [1 – 3]. In addition to these applications, the hybrid filter bank (HFB) is suitable for high resolution conversion between continuous-time and digital signals. The HFB associated also with analog to digital conversion working at lower sample rates in comparison with the Nyquist sampling rate of the input signal [4 – 8]. They are inspired from perfect or near perfect reconstruction digital filter bank that use digital filter for both analysis and synthesis filter bank. Several methods have been developed using IIR digital filters to design filter bank [9 – 12]. Thus, the HFBs are an unconventional class of the filter banks that employs both analog and digital filters [13 – 15]. Their sensitivity to aliasing and mismatch, component tolerances, will have a strong impact on analysis property of the filter bank and thus on the performances of the continuous-time to digital conversion process.

[1]University of Niš, Faculty of Electronic Engineering, Aleksandra Medvedeva 14, 18000 Niš, Serbia; E-mails: vidosav.stojanovic@elfak.ni.ac.rs; nikola.stojanovic@elfak.ni.ac.rs
[2]University of Priština (at K. Mitrovica) Faculty of Natural Science, 28220 Kosovska Mitrovica, Lole Ribara 29, Serbia; e-mail: negovan.stamenkovic@pr.ac.rs

The principle of a continuous-time linear hybrid two channel filter bank is shown in Fig. 1. The system consists an continuous-time analysis two channel filter bank, uniform samplers, quantizers, upsampler and a discrete-time synthesis filter bank. The input continuous-time signal $x(t)$ is supposed to be strictly bandlimited to π / T_s, where T_s is the sample period of the system. In this case, the Nyquist criterion for sampling with an effective sampling period of T_s without aliasing is fulfilled.

The analysis filter bank consists of the low-pass filter $H_0(s)$ and high-pass filter $H_1(s)$. Both filters have the same pass-band edge and split the spectrum of the band limited input signal $x(t)$ by the factor of 2. The sampling and quantization takes place at the output of the analysis filters with the twice lower sampling frequency $1/(2T_s)$. The quantized signal goes into a linear discrete-time synthesis filter bank, which generate a single signal $y(n)$ from upsampled by and interpolated signals. The up samplers are used to retain the desired Nyquist sampling rate $1/T_s$.

The synthesis filter bank is formed by discrete-time synthesis filters $F_0(z)$ and $F_1(z)$. It is known that discrete-time IIR filters of odd degree can be realized as the sum of two stable all-pass filters with real coefficients having no common poles [16 – 18]. It is known that discrete-time synthesis filter bank composed of two real allpass filters can be implemented with low complexity structures that are robust to the finite word length. The continuous-time filters chosen to build the analysis filter bank play an important role in the performance of the hybrid filter bank. Furthermore, two channel hybrid filter bank can be easy used for design *K*-channel hybrid filter bank based on a tree structure.

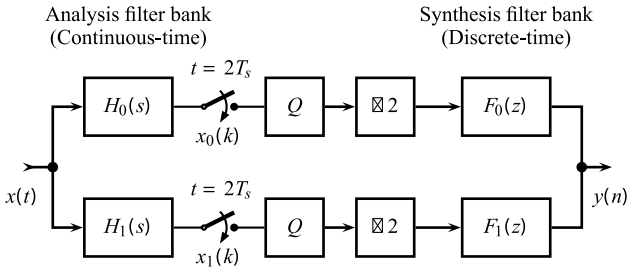

Fig. 1 – *Two channel hybrid continuous/discrete time filter bank.*

For the definition purposes, consider a continual prototype lowpass-highpass filter pair, denoted by $[H_0(s), H_1(s)]$, where $H_0(s)$ is transfer function of lowpass part of filter pair and $H_1(s) = H_0(s^{-1})$ is transfer function of

highpass part filter pair. Normalized passband edge for both filters is equal to one.

A filter pair $[H_0(s),H_1(s)]$ is a *power-complementary* filter pair [19] if the sum of the squares of their magnitude responses satisfies

$$H_0(s)H_0(-s)+H_1(s)H_1(-s)=1\,, \tag{1}$$

or at real frequency $s=\mathrm{j}\omega$

$$|H_0(\mathrm{j}\omega)|^2+|H_1(\mathrm{j}\omega)|^2=1\,. \tag{2}$$

For this pair, the angular frequency $\omega_c=1$, where $|H_0(\mathrm{j})|^2=|H_1(\mathrm{j})|^2=0.5$, is the *crossover angular frequency*. At this angular frequency, the gain responses of both filters are approximately 3 dB below their maximum values. Note, crossover angular frequency is 3 dB passband edge for both lowpass and highpass part of filter pair.

A filter pair $[H_0(s),H_1(s)]$ is an *all-pass-complementary* filter pair [20] if the sum and difference of $H_0(s)$ and $H_1(s)$ satisfies

$$\begin{aligned} H_0(s)+H_1(s)&=A_1(s)\\ H_0(s)-H_1(s)&=A_2(s) \end{aligned} \tag{3}$$

where $A_1(s)$ and $A_2(s)$ are all-pass transfer functions.

Transfer function sets which are simultaneously all-pass complementary and power complementary are termed *doubly complementary*. All doubly complementary filter pair can be expressed as the sum of stable allpass filters such as the Butterworth and the elliptic filters. The other classical approximation cannot form a double complementary pair.

New efficient approximation of the continuous-time doubly complementary filter pair is proposed in this paper. The realization, based on the continuous-time allpass filters, which validate this approach is also presented.

Rational Transfer Function

The necessary and sufficient conditions for the rational transfer function to be suitable for the realization of the continuous-time two channel filter banks are given in this section. In general, the squared magnitude characteristic of the lowpass prototype in the *s*-plane is expressed in the form known as Feldtkeller equation [21, pp. 196-204]:

$$H(s)H(-s)=\frac{1}{1+K(s)K(-s)}\,, \tag{4}$$

where the filter characteristic function $K(s)$ is a rational function with real coefficients. Since poles of characteristic function are zeros of the transfer function, the polynomial in the denominator of characteristic function contains only even power of *s*, but the polynomial in nominator may contain either an only even or only odd power of *s*. For power symmetric filter design, at normalized passband edge frequency $s = \pm \mathrm{j}$ the characteristic function is equal to one, then the insertion loss of filter at this frequency is 3.0103 dB. In fact, Butterworth, Chebyshev1, Chebyshev2, and elliptic filters are introduced in this form, and the filter properties are governed in a way where $K(s)$ is chosen [22]. Only Butterworth and elliptic filters satisfy all-pass complementary and power complementary properties. Therefore, the approximation problem is to find the real coefficient characteristic function such that the resulting transfer function can be represented as an all-pass complementary filter pair.

The following text presents the conditions that should satisfy the rational form $K(s)$ which make $H(s)$ as a double complementary filter pair.

Lemma 1. *The rational transfer functions* $H_0(s) = H(s)$ *and* $H_1(s) = H(1/s)$ *in (1) satisfied power symmetric s-domain if*

$$K(s)K(-s)K(s^{-1})K(-s^{-1}) = 1. \tag{5}$$

Proof. Since this property in the *z*-domain is satisfied [23], we will show that this property also satisfied is in the *s*-domain. For (4) we have

$$\begin{aligned} & H(s)H(-s) + H(s^{-1})H(-s^{-1}) \\ &= \frac{1}{1+K(s)K(-s)} + \frac{1}{1+K(s^{-1})K(-s^{-1})} \\ &= \frac{1+R(s)}{R(s)+K(s)K(-s)K(s^{-1})K(-s^{-1})}, \end{aligned} \tag{6}$$

where $R(s) = 1 + K(s)K(-s) + K(s^{-1})K(-s^{-1})$. Clearly, this is equal to one if and only if

$$K\left(s\right)K\left(-s\right)K\left(s^{-1}\right)K\left(-s^{-1}\right) = 1.$$

This lemma is proved.

Based on the preceding result it is possible to develop a general analytic form for $K(s)$ which is suitable for continuous-time power symmetric filter design.

Lemma 2. *A rational filter transfer function (4) satisfied power symmetric in the s-domain (5) if and only if characteristic function has the form*

$$K(s) = s^k \prod_{m=1}^{M} \left(\frac{s^2 + \omega_m^2}{\omega_m^2 s^2 + 1} \right)^{l_m}, \tag{7}$$

with zeros at $\omega_m < 1$, *poles at* $1/\omega_m > 1$ *and arbitrary integer* l_m, *for* $m = 1, 2, \ldots, M$. *Filter order is* $N = k + 2\sum_{m=1}^{M} l_m$.

This condition can be expressed equivalently by

$$K(-s)K(s^{-1}) = (-1)^k \tag{8}$$

for all s.

Proof. This comes from the solution in the *z*-domain [24] based on the following facts:

1. $K(-s) = (-1)^k K(s)$,
2. $K(s^{-1}) = \dfrac{1}{K(s)}$.

This lemma is proved.

The problem now is to find the location of the pole or zero factors such that equiripple behavior is achieved in both the passband and the stopband.

Note, for $k > 1$ and $l_1 = l_2 = \cdots = l_M = 0$ we have Butterworth filter which is power-symmetric. For $k = 0$ or 1 and $l_1 = l_2 = \cdots = l_M = 1$ we have Elliptic filters which is also power-symmetric. Chebyshev filters cannot be power-symmetric because they have ripples only in the passband or stopband.

Lemma 3. Let $H(s)$ be a rational with real coefficients power symmetric filter function, then all poles of it are restricted to be on the unit circle.

Proof. Since $K(s)$ has the form (7), its poles are restricted to be on the imaginary axis, then power symmetric $H_0(s)$ implies (8) and (4) can be rewritten as

$$H(s)H(-s)=\frac{1}{1+(-1)^k\dfrac{K(s)}{K(s^{-1})}}. \tag{9}$$

At pole frequencies of $H(s)$ the denominator of the expression (9) is zero, that is

$$\frac{K(s)}{K(s^{-1})}=(-1)^{k+1}. \tag{10}$$

In view of the real-coefficient assumption at $s=\mathrm{e}^{\mathrm{j}\theta}$ we have $K(\mathrm{e}^{-\mathrm{j}\theta})=K^*(\mathrm{e}^{\mathrm{j}\theta})$, where K^* is conjugate of *K*. On the unit circle in the *s*-plane we therefore have

$$\left|\frac{K(\mathrm{e}^{\mathrm{j}\theta})}{K^*(\mathrm{e}^{\mathrm{j}\theta})}\right|=1. \tag{11}$$

So, the quantity $K(s)/K(s^{-1})$ has unit-magnitude on the unit circle, then all poles of $H(s)H(-s)$ are on the unit circle. Thus, the denominator of $H(s)$ is a mirror image polynomial, which satisfies the following condition $p_n(s)=s^n p_n(1/s)$.

Lemma 4. *A filter pair* $[H_0(s),H_1(s)]$, *where* $H_0(s)=H(s)$ *and* $H_1(s)=H(s^{-1})(s)$, *is an all-pass-complementary filter pair of transfer functions, i.e., a par satisfied*

$$H_0(s)+H_1(s)=A_1(s), \tag{12}$$

where $A_1(s)$ is an stable all-pass transfer function. Then, the following equation is also automatically satisfied

$$H_0(s)-H_1(s)=A_2(s). \tag{13}$$

Proof. Since $A_1(s)$ and $A_2(s)$ are the allpass transfer functions, then $A_1(s)A_1(-s)=1$ and $A_2(s)A_2(-s)=1$. Further, the squared magnitude characteristic of the left side of (12) is

$$\begin{aligned}G(s)=[H_0(s)+H_1(s)][H_0(-s)+H_1(-s)]=\\ 1+H_0(s)H_1(-s)+H_0(-s)H_1(s).\end{aligned} \tag{14}$$

because filter pair $[H_0(s),H_1(s)]$ is power complementary.

Let *N* be odd. Transfer function $H_0(s)$ and $H_1(s)$ have the form

$$H_0(s)=\frac{\prod_{m=1}^{M}(\omega_m^2 s^2+1)^{l_m}}{(s+1)(s^{N-1}+\alpha_1 s^{N-2}+\cdots+\alpha_1 s+1)},$$
$$H_1(s)=\frac{s^{N-2\nu}\prod_{m=1}^{M}(s^2+\omega_m^2)^{l_m}}{(s+1)(s^{N-1}+\alpha_1 s^{N-2}+\cdots+\alpha_1 s+1)}, \tag{15}$$

where $\nu=\sum_{m=1}^{M} l_m$ and $N=k+2\nu$. Since $H_0(s)$ is a ratio of even and odd polynomials then $H_0(-s)=-H_0(s)$. On the other hand, $H_1(s)$ is a ratio of odd polynomials then $H_1(-s)=H_1(s)$. When this is substituted into equation (14), we obtain $G(s)=1$, i.e., squared magnitude characteristic of $H_0(s)+H_1(s)$ is equal to one. Thus, $H_0(s)+H_1(s)$ is an allpass function.

In the same way one can show that $H_0(s)-H_1(s)$ is also allpass function.

3 The Two Channel Continuous-Time Filter Bank

Two-channel power complementary continuous-time filter bank [25 – 27] shown in Fig. 2 is considered in this section, where $A_1(s)$ and $A_2(s)$ are two continuous time stable all-pass filters with real coefficients having no common poles.

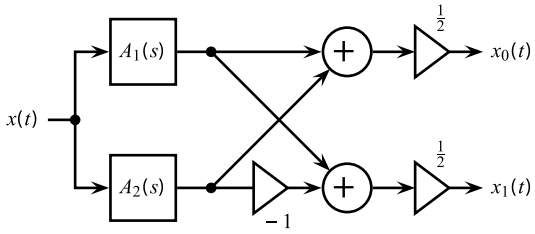

Fig. 2 – *The system of two-channel power complementary filter bank.*

It is interesting to note that only continuous-time filters of odd degree can be realized as a real coefficient all-pass sum. Transfer function of the lowpass filter is

$$H_0(s)=\frac{X_0(s)}{X(s)}=\frac{1}{2}[A_1(s)+A_2(s)] \tag{16}$$

and of the highpass filter

$$H_1(s) = \frac{X_1(s)}{X(s)} = \frac{1}{2}[A_1(s) - A_2(s)]. \tag{17}$$

The transfer functions $H_0(s)$ and $H_1(s)$ can be implemented simply by implementing all-pass networks $A_1(s)$ and $A_2(s)$. In the following, we use $A_{1,2}(\mathrm{j}\omega) = \mathrm{e}^{-\mathrm{j}\phi_{1,2}(\omega)}$, where $\phi_{1,2}(\omega)$ is the phase frequency response of the all-pass network and $s = \mathrm{j}\omega$ denotes normalized angular frequency. Therefore, we have the frequency response of lowpass filter

$$H_0(\mathrm{j}\omega) = \cos\left[\frac{\phi_1(\omega) - \phi_2(\omega)}{2}\right] \mathrm{e}^{-\mathrm{j}\frac{\phi_1(\omega)+\phi_2(\omega)}{2}} \tag{18}$$

and of the highpass filter

$$H_0(\mathrm{j}\omega) = \mathrm{j}\sin\left[\frac{\phi_1(\omega) - \phi_2(\omega)}{2}\right] \mathrm{e}^{-\mathrm{j}\frac{\phi_1(\omega)+\phi_2(\omega)}{2}}. \tag{19}$$

The magnitude frequency response of the filters is determined by the difference of allpass phases, and the phase frequency response of the filters is given by the sum of the allpass phases.

3.1 Approximation

The magnitude-squared response of the proposed *N*-th degree characteristic function (7) with multiple pair of zeros ($\omega_1 = \omega_2 = \cdots = \omega_M = \omega_0$ and $l_1 = l_2 = \ldots = l_M = 1$) on the imaginary axis at real frequencies $\pm\mathrm{j}\omega_0$ has the form

$$K(\omega) = \omega^k \left(\frac{\omega^2 - \omega_0^2}{\omega^2\omega_0^2 - 1}\right)^M,$$

where $\omega_0 < 1$, the filter degree is $N = k + 2M$. The magnitude squared transfer function is given by the equation (4) which at real frequencies $s = \mathrm{j}\omega$ has the form

$$|H(\mathrm{j}\omega)|^2 = \frac{1}{1 + \omega^{2k}\left(\frac{\omega^2 - \omega_0^2}{\omega^2\omega_0^2 - 1}\right)^{2M}}. \tag{20}$$

Fig. 3 shows frequency response of proposed characteristic function for $k = 3$ and $M = 3$. The left branch of the characteristic function is enlarged 10^4 times. The minimum characteristic function in the stopband is $K_{min} = 177.82512$ times. On the other hand, the maximum characteristic function in the passband is only 0.005628 times. It should be noted that the

characteristic function has only one ripple both in the passband and in the stopband.

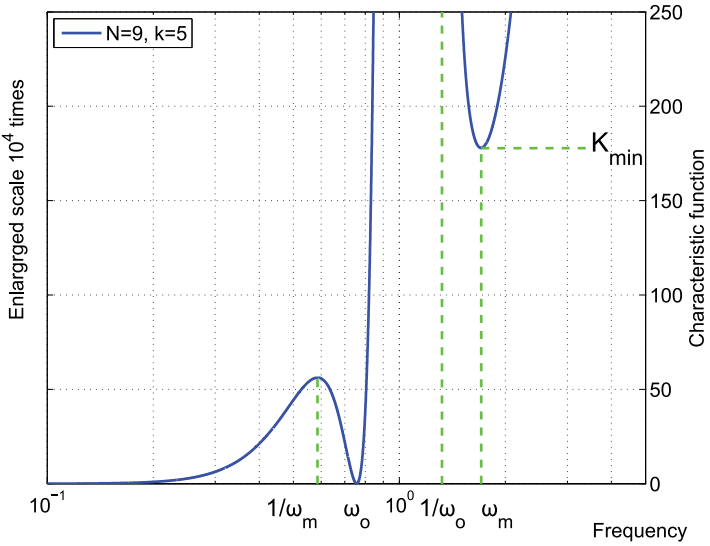

Fig. 3 – *Characteristic function for k = 5 and M = 2.*

Unknown frequency ω_0 should be determined so that the minimum attenuation a_{min} at frequency ω_m in the stop-band has proposed value. Therefore, two unknown frequencies ω_0 and ω_m can be determined by solving two nonlinear equations:

$$f_1(\omega_0,\omega_m)=\frac{\mathrm{d}\,K(\omega_m)}{\mathrm{d}\,\omega_m}=0,$$
$$f_2(\omega_0,\omega_m)=K(\omega_m)-a_{min}=0. \tag{21}$$

Newton-Raphson algorithm [28, 29] is applied to solve the system of two nonlinear equations (21). In this method two initial value $\omega_0^{(0)}$ and $\omega_m^{(0)}$ are required. First for multiple zero and second for frequency at which the minimum stop-band attenuation occur

$$\begin{bmatrix}\omega_m^{(i+1)}\\ \omega_0^{(i+1)}\end{bmatrix}=\begin{bmatrix}\omega_m^{(i)}\\ \omega_0^{(i)}\end{bmatrix}-\begin{bmatrix}\dfrac{\partial f_1(\omega_m,\omega_0)}{\partial\omega_m} & \dfrac{\partial f_1(\omega_m,\omega_0)}{\partial\omega_0}\\ \dfrac{\partial f_2(\omega_m,\omega_0)}{\partial\omega_m} & \dfrac{\partial f_2(\omega_m,\omega_0)}{\partial\omega_0}\end{bmatrix}^{-1}\times\begin{bmatrix}f_1\\ f_2\end{bmatrix}. \tag{22}$$

Since the minimum stopband attenuation R_s is given in dB, then $a_{min} = \sqrt{10^{R_s/10} - 1}$ times. A convergence criterion could be that the maximum of the absolute values of the functions f_i, $i = 1,2$ is smaller than a certain tolerance ε, i.e.,

The result is obtained after a few iterations.

$$\max_{i=1,2} | f_i(\omega_0, \omega_m) | < \varepsilon . \tag{23}$$

Performing analytic continuation $\omega = -\mathrm{j}s$, equation (20) gets the form

$$H(s)H(-s) = \frac{(\omega_0^2 s^2 + 1)^{2M}}{(\omega_0^2 s^2 + 1)^{2M} + (-1)^k s^{2k} (s^2 + \omega_0^2)^{2M}} . \tag{24}$$

Poles of the magnitude-squared transfer function (24) are zeros of the denominator

$$(-1)^k s^{2k} (s^2 + \omega_0^2)^{2M} + (\omega_0^2 s^2 + 1)^{2M} = 0 . \tag{25}$$

The symbolic tool (Matlab or Matematica) can be performed to find the roots of the equation (25). However, the polynomial (25) is image mirror polynomial which can be rewritten in following form

$$d_0 s^{2(k+2M)} + d_2 s^{2(k+2M-1)} + \cdots + d_2 s^2 + d_0 = 0 , \tag{26}$$

where

$$d_{2i} = \begin{cases} \binom{2M}{i} (\omega_0^2)^i , & i = 0, \ldots, k-1, \\ \binom{2M}{i} (\omega_0^2)^i + (-1)^k \binom{2M}{i-k} (\omega_0^2)^{2M-i+k}, & i = k, \ldots, 2M, \\ (-1)^k \binom{2M}{i-k} (\omega_0^2)^{2M-i+k}, & i = 2M+1, \ldots, 2M+k. \end{cases} \tag{27}$$

Since the transfer function is stable, its poles will be those of the magnitude-squared transfer function that lie in the left half plane of complex frequency space. The transfer function is given by

$$H(s) = \frac{(\omega_0^2 s^2 + 1)^M}{s^N + a_2 s^{N-1} + a_3 s^{N-2} \cdots + a_3 s^2 + a_2 s + 1} . \tag{27}$$

Using the described procedure, transfer functions for $n = 7$ and for three different values of flatness at origin, $k = 1,3,5$, have been determined and the

results in factored second degree form[3] are listed in **Table 1**. Since the minimum stopband attenuation is 40 dB then passband ripple is 4.3432×10^{-4} dB. The frequency scale is normalized so that $\omega_{3dB}=1$.

Table 1

Double complementary approximation function for R_p = 40 dB.

k	Denominator of $H(s)$	Numerator of $H(s)$
5	$(s+1)(s^2+1.713603s+1)(s^2+1.019803s+1)(s^2+0.306200s+1)$	$0.464904s^2+1$
3	$(s+1)(s^2+1.545325s+1)(s^2+0.760800s+1)(s^2+0.215475s+1)$	$(0.496681s^2+1)^2$
1	$(s+1)(s^2+1.438917s+1)(s^2+0.715139s+1)(s^2+0.214115s+1)$	$(0.396015s^2+1)^3$

The transfer function can be represented as a product of second order transfer functions with equal pole frequency $\omega_p=1$. Pole quality factor of each second order section is the reciprocal of the linear term coefficient. It can be shown, that when k decrease, then critical pole quality factor q_c increase.

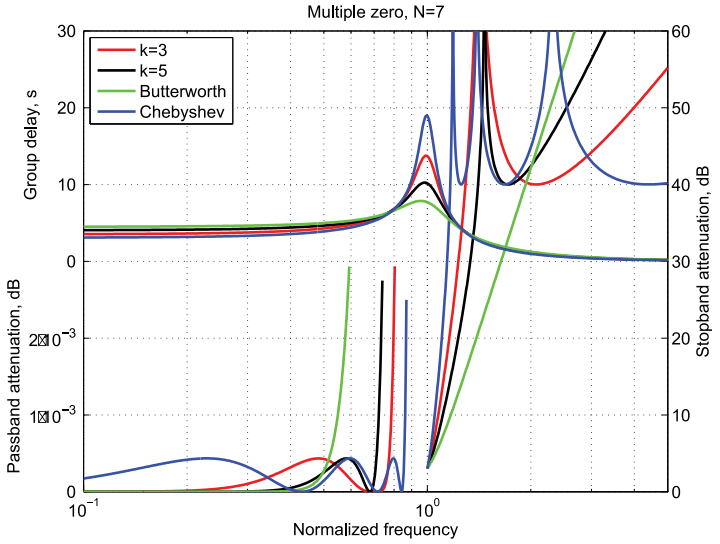

Fig. 4 – *Magnitude and group delay characteristics of the seventh-degree Butterworth and elliptic filters compared with filters of the new design for* k = 3 *and* k = 5.

[3]Second degree factor can be written in following form [30]

$$s^2+\frac{\omega_p}{q}s+\omega_p^2$$

where ω_p represents pole frequency and q refers to the pole quality factor.

In the illustration in Fig. 4 the seventh order Butterworth filter and elliptic filter with minimum stopband attenuation of 40 dB are compared with two corresponding filters of proposed design which have three ($k = 3$) and five ($k = 5$) flatness at origin. It is well known that the performances of all allpole and rational approximations lie between Butterworth and elliptc approximation. The aim of this comparison is to show the position of the proposed approximation in the area between these two approximations.

The critical pole quality factor of proposed approximation increases if flatness at origin decreases, and for nine degree new approximation for $k = 1$ and $a_{\min} = 40$ dB it is 4.6704. These values lie also between Butterworth and elliptic approximation. Critical pole quality factor for Butterworth and elliptic filter with 40 dB minimum stopband attenuation are 2.2469797 and 6.7540917, respectively.

Table 2

All-pass sections A_1 and A_2 for realization analysis part of hybrid filter bank.

k		Denominator	Numerator
5	A_1	$(s^2 + 1.713603s + 1)(s^2 + 0.306200s + 1)$	$(s^2 - 1.713603s + 1)(s^2 - 0.306200s + 1)$
	A_2	$(s + 1)(s^2 + 1.019803s + 1)$	$(-s + 1)(s^2 - 1.019803s + 1)$
3	A_1	$(s^2 + 1.545325s + 1)(s^2 + 0.215475s + 1)$	$(s^2 - 1.545325s + 1)(s^2 - 0.215475s + 1)$
	A_2	$(s + 1)(s^2 + 0.760800s + 1)$	$(-s + 1)(s^2 - 0.760800s + 1)$
1	A_1	$(s^2 + 1.438917s + 1)(s^2 + 0.214115s + 1)$	$(s^2 - 1.438917s + 1)(s^2 - 0.214115s + 1)$
	A_2	$(s + 1)(s^2 + 0.715139s + 1)$	$(-s + 1)(s^2 - 0.715139s + 1)$

The all-pass sections, which are used to realize the analysis part of the HFB are listed in **Table 2** in factored form. The denominator polynomial in the all-pass sections is a Hurwitz polynomial, but the nominator polynomial has right-half plane zeros that are mirror images around the imaginary axis of left-half plane poles.

Pole-zero plot of transfer function and its two allpass functions are shown in Fig. 5. Poles of all-pass functions are at the same time the poles of the transfer function.

In $A_1(s)$ are included the outermost pole pair, the third outermost pole pair, and so on (see the pole pair tagged with $\times$ on the Fig. 5). The remaining pole pairs belong to $A_2(s)$.

The transfer function of an even degree is not suitable for complementary decomposition because it allpass transfer functions have complex coefficients. Therefore the order of allpass subfilters must differ by 1.

4 Implementation

In this section we discuss the design of continuous-time part of two channel hybrid filter bank based on all-pass active RC structure. All-pass transfer functions are non-minimum phase transfer function i.e., they have zeros in the right half of the complex-frequency plane.

Basically, there are two implementation manners of realizing such continuous-time allpass filter circuits. One alternative is the passive implementation, consisting of only passive components like capacitors and inductors. A number of passive circuit topologies exist, which can be used for this purpose, for instance the second-degree all-pass lattice structure with constant resistance properties or bridged-T structures [31].

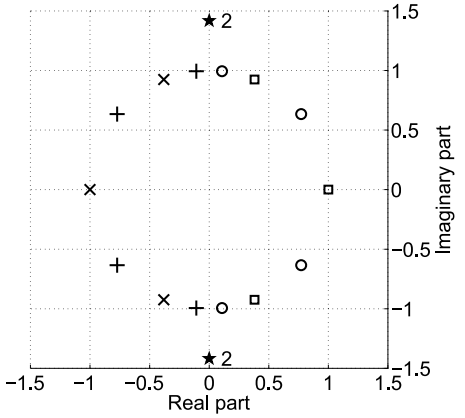

Fig. 5 – *Pole-zero plot of allpass functions in s-plane of the 7th-order prototype for transfer function with* R_s = 40 dB, M = 1 and l_1 = 2. *Poles and zeros of* $A_1(s)$ *are tagged with* + *and* ○ *respectively*; *but poles and zeros of* $A_2(s)$ *are tagged with* × *and* □ *respectively*. *The transfer function zeros are tagged with* ★. *The number* 2 *indicates that it is double-zero.*

The other alternative is the active implementation, consisting of active devices like operational amplifiers, operational transconductance amplifier [32] or current conveyor [33, 34]. Through the application of active components, it is possible to omit the bulky and costly inductor components, as well as provide more freedom in the shaping of the filter characteristic. The active RC realization by cascading first and second order section (biquad) is proposed in this paper. The biquad can be realized with single or more operational amplifiers. The single amplifier biquad (SAB) lowpass and highpass filter will be discussed in this section. The SAB networks are canonic because these employ two capacitors only.

The continuous-time part of hybrid filter bank is initially designed for a normalized frequency $\omega_c = 1$, and then frequency transformation is performed to obtain the desired ω_c. Impedance scaling may also be applied for more convenient component values.

The single amplifier all-pass network first degree and the Delyiannis second degree multiple feedback all-pass network are given in the Figs. 6a and 6b, respectively [35, chap. 4]. It is assumed that the ideal operational amplifiers are used. This all-pass type can be used for section Q-factor between 0 and 20, and it does not provide gain. The basic aim is to implement the circuits of Fig. 6 in one operational amplifier.

The circuit on the Fig. 6a is referred as the first-degree grounded capacitor allpass network that implements one real pole and one real zero. The transfer function for the circuit shown in Fig. 6 is as follows:

$$H(s) = \frac{R_2}{R_1} \frac{-s + \dfrac{1}{RC}\dfrac{R_1}{R_2}}{s + \dfrac{1}{RC}}. \tag{28}$$

For $R_1 = R_2$ pole and zero frequency are equal then the transfer function is first degree allpass network.

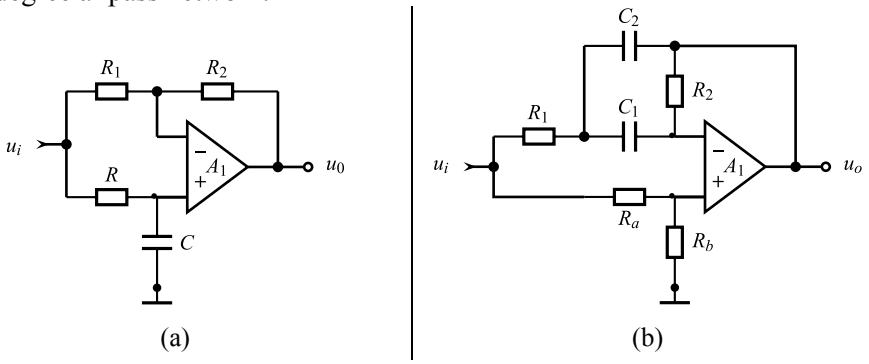

Fig. 6a – (a) *The single amplifier all-pass network first degree*, *and* (b) *the single amplifier all-pass network second degree.*

Transfer function of allpass network second degree, assuming ideal operational amplifier, is as follows

$$H(s) = h_o \frac{s^2 - \left[\dfrac{R_a}{R_b}\dfrac{1}{R_1C_2} - \dfrac{C_1 + C_2}{R_2C_1C_2}\right]s + \dfrac{1}{R_1R_2C_1C_2}}{s^3 + \dfrac{C_1 + C_2}{R_2C_1C_2}s + \dfrac{1}{R_1R_2C_1C_2}}, \tag{29}$$

where $h_o = R_b / (R_a + R_b)$ is the feedforward gain which is less than one. As for initial circuit component values the value $C_1 = C_2$ is used. It is recognized that (see **Table 2**) pole quality factor, q_p, and pole frequency, $\omega_p = 1$, are

$$\frac{1}{q_p} = \frac{C_1 + C_2}{R_2 C_1 C_2} \quad \text{and} \quad \omega_p = \frac{1}{R_1 R_2 C_1 C_2}. \tag{30}$$

Since experience has indicated that required *Q*-factors are usually well under 20, then network shown in Fig. 6b is suffice in this implementation.

From (30) we obtain the following initial circuit component values

$$R_1 = \frac{1}{2Cq_p}, \quad R_2 = \frac{2q_p}{C}, \quad \frac{R_a}{R_b} = 4\frac{R_1}{R_2} \tag{31}$$

Fig. 7 shows the nine-degree two channel continuous-time filter bank using first and second degree single amplifier all-pass section given in Fig. 6. This scheme does not require the trimming of capacitors because the measured values of the capacitors can be used to compute the values of the resistors which are then trimmed to the desired values.

The low-pass prototype that will be used to design two channel filter bank is:

$$H(s) = \frac{(0.6146718s^2 + 1)^3}{(s+1)(s^2 + 1.56517s + 1)(s^2 + 0.83718s + 1)} \cdot \frac{}{(s^2 + 0.38532s + 1)(s^2 + 0.11331s + 1)} \tag{32}$$

The transfer function (32) is decomposed into two real all-pass functions $A_1(s)$ and $A_2(s)$

$$A_1(s) = \frac{(-s+1)(s^2 - 0.83718s + 1)(s^2 - 0.11331s + 1)}{(s+1)(s^2 + 0.83718s + 1)(s^2 + 0.11331s + 1)} \tag{33}$$

and

$$A_2(s) = \frac{(s^2 - 1.56517s + 1)(s^2 - 0.38532s + 1)}{(s^2 + 1.56517s + 1)(s^2 + 0.38532s + 1)}. \tag{34}$$

The first all-pass filter $A_1(s)$ is realized by one first order section shown in Fig. 6a and two second order sections shown in Fig. 6b and placed in cascade. The second all-pass filter $A_2(s)$ is realized by two second order section placed in in cascade. Since the dc gain, which is realized by using all-pass section A_1 and A_2, is less than one, then the output voltages are scaled by using noninverting amplifiers so that whole dc gain, from input $x(t)$ to both outputs $v_1(t)$ end $v_2(t)$ is equal to one.

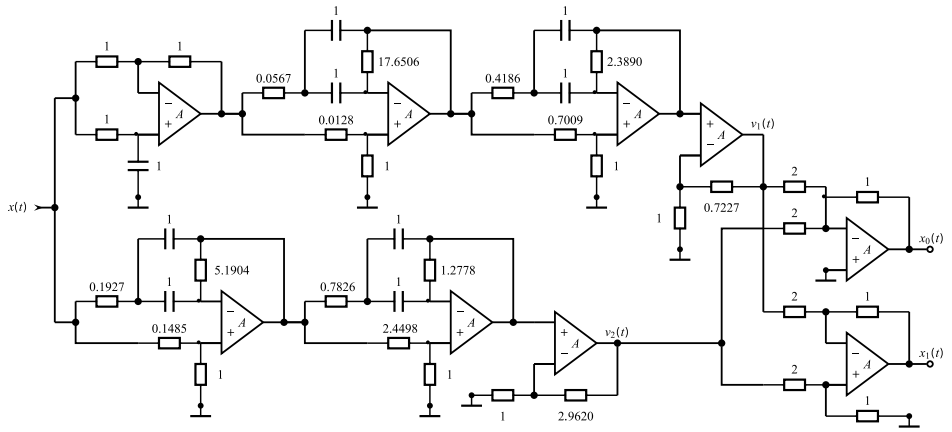

Fig. 7 – *Implementation of nine degree continuous-time part of two channel hybrid filter bank.*

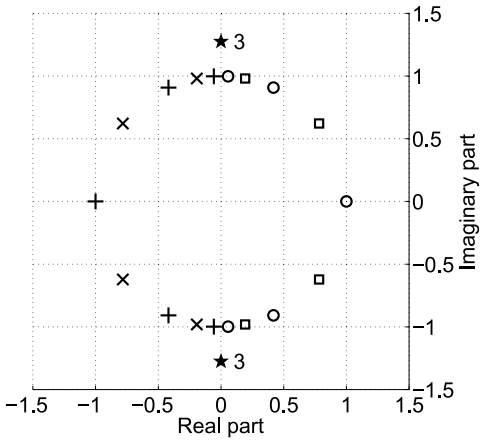

Fig. 8 – *Pole-zero plot of allpass functions in s-plane of the 9th-order prototype for transfer function with* R_s = 40 dB, M = 1 and l_1 = 3. *Poles and zeros of* $A_1(s)$ *are tagged with* + *and* ○ *respectively*; *but poles and zeros of* $A_2(s)$ *are tagged with* × *and* □ *respectively*. *The transfer function zeros are tagged with* ★. *The number* 3 *indicates that it is triple-zero.*

The standard scaling summing amplifier is used to summing output voltages $v_1(t)$ and $v_2(t)$ of all-pass networks A_1 and A_2 respectively. Both input variables are scaled with the same factor (–0.5). Note that this network inverts the input signals.

As the subtractor circuit the standard difference amplifier is used. The output voltage $v_1(t)$ is applied to the inverting terminal and the output voltage $v_2(t)$ to the non-inverting terminal. The difference amplifier gain is 0.5. In this way, the $x_0(t)$ and $x_1(t)$ are obtained as an inverted value.

We have to perform a simulation of the two channel continuous-time filter bank with component values shown in Fig. 7. Pole-zero plot is given in the Fig. 8. The transfer function poles are tagged with × and +, and multiple zero is tagged with ★. The number 3 indicates that it is triple-zero. Zeros tagged with ○ an □ are are related to all-pass function $A_1(s)$ and $A_2(s)$, respectively.

The lowpass and highpass impulse responses for a nine-degree proposed analysis filter bank can be seen in Fig. 9. The picture shows the ideal impulse response and impulse response when the component filters are rounded to the three digits. The error which results from quantizing the component values to 3 digits also shown in Fig. 9, where it can be seen that three digits are sufficient to maintain an impulse response error less than 0.004 for both impulse responses.

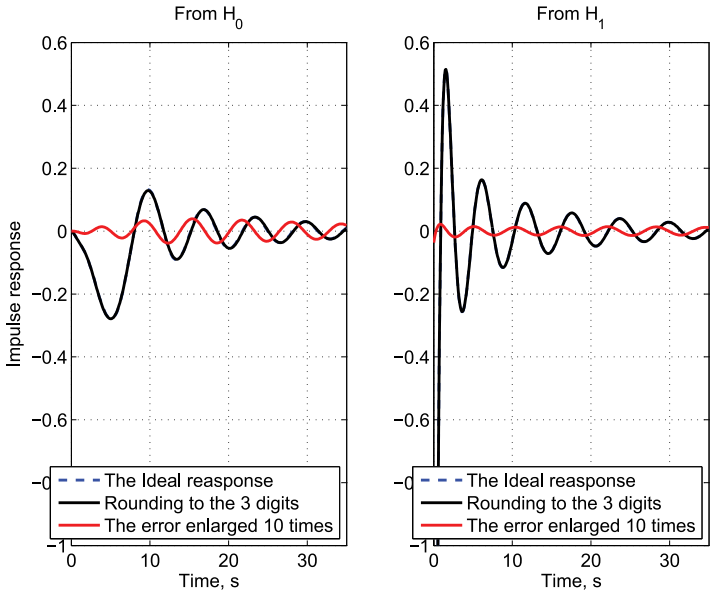

Fig. 9 – *Impulse responses for N* = 9: (a) *Lowpass filter*, (b) *highpass filter.*

Better results can be obtained by trimming resistors of the filter so that at the phase difference at a frequency of the zero ω_0 between $v_1(t)$ and $v_2(t)$ is π radians. Trimming of all-pass sections A_1 and A_2 is usually done by successively

applying a sinusoidal input signal at frequency ω_0 (normalized value is 1.257) and measuring the phase difference of the output signals. The Lissajous figure can be used for easy find π radians phase shift [36]. Lissajous figure is obtained with the oscilloscope in its *x*-*y* mode with the output $v_1(t)$ tied to the *x* channel and the output $v_2(t)$ tied to the *y* channel.

Other architecture can be used for the second degree all-pass filter implementation. For example, a class of biquadratic building blocks with two operational amplifiers can be used for the implementation of all-pass function [37]. This dual amplifier biquads is particularly favorable for practical applications.

5 Conclusion

A new class of continuous-time filter structures has been presented, which can be used for efficient implementation of the hybrid two channel filter bank. The conditions required to be satisfied by the transfer functions, so as to two channel filter bank can be implemented as a parallel connection of two all-pass filters, are listed. The transfer function is characterized by multiple zero at real frequencies in the stopband. The multiplicity of zero acts as free parameter which can adjust selectivity of the filter.

If filter degree is odd, all-pass functions have real coefficients, but for even filter degree the all-pass function involve the implementation the complex coefficients.

The proposed filter approximation of degree nine as all-pass sum is implemented. The all-pass filter is formed as the cascade of first and second degree sections. The Delyiannis single amplifier second degree all-pass network is used to implemented second degree sections. The finite gain-bandwidth product of the operational amplifier is not analyzed.

The efficiency of the proposed design has been demonstrated by means of an complete design example. The nine-degree filter using simple amplifier biquad for design all-pass sections is implemented. It is shown that rounding component values to three digits produces impulse response absolute error less than 0.004.

6 Acknowledgment

This work is supported by Serbian Ministry of Science and Technologies, Project No. 32009TR.

7 References

[1] L. Cohen: Time-frequency Distributions - A Review, Proceedings of the IEEE, Vol. 77, No. 7, July 1989, pp. 941 – 981.

[2] Z. Xizheng, Y. Ling, W. Weixiong: Wavelet Time-frequency Analysis of Electroencephalogram (eeg) Processing, International Journal of Advanced Computer Science and Applications, Vol. 1, No. 5, Nov. 2010, pp. 1 – 5.

[3] J. Han, M. van der Baan: Empirical Mode Decomposition for Seismic Time-frequency Analysis, Geophysics, Vol. 78, No. 2, March/April 2013, pp. O9 – O19.

[4] J.L. Collette, M. Barret: On Simulations about the Precision of Non Uniform Hybrid Filter Bank Analog/Digital Converters, IEEE International Conference on Acoustics, Speech and Signal Processing, Toulouse, France, 14 – 19 May 2006, Vol. 3, pp. III 237 – III 240.

[5] D. Asemani, J. Oksman, P. Duhamel: Subband Architecture for Hybrid Filter Bank A/D Converters, IEEE Journal of Selected Topics in Signal Processing, Vol. 2, No. 2, Apr. 2008, pp. 191 – 201.

[6] B. Szlachetko, O. Venard: Hybrid Filter Bank Design and Analysis, Signal Processing: Algorithms, Architectures, Arrangements and Applications, Poznan, Poland, 26 – 28 Sept. 2013, pp. 129 – 132.

[7] Y. Chunyan: A Modulated Hybrid Filter Bank for Wide-band Analog-to-digital Converters, Journal of Multimedia, Vol. 9, No. 4, Apr. 2014, pp. 569 – 575.

[8] W. Wang, Z.J. Zhang: Design of Digital Synthesis Filters for Hybrid Filter Bank A/D Converters using Semidefinite Programming, Journal of Networks, Vol. 9, No. 5, May 2014, pp. 1325 – 1332.

[9] P. Vaidyanathan, S. Mitra, Y. Neuvo: A New Approach to the Realization of Low-sensitivity IIR Digital Filters, IEEE Transactions on Acoustics, Speech and Signal Processing, Vol. 34, No. 2, Apr. 1986, pp. 350 – 361.

[10] J. Upendar, C.P. Gupta, G.K. Singh: Designing of Two Channel Quadrature Mirror Filter Bank using Partical Swarm Optimization, Digital Signal Processing, Vol. 20, No. 2, March 2010, pp. 304 – 313.

[11] N. Stamenkovic, V. Stojanovic: The Design of Two Channel IIR QMF Bank Directly from Analog Prototype, International Journal of Electronics, Vol. 98, No. 7, July 2011, pp. 961 – 972.

[12] P. Ghosh, S. Das, H. Zafar: Adaptive-differential-evolution-based Design of Two-channel Quadrature Mirror Filter Banks for Sub-band Coding and Data Transmission, IEEE Transactions on Systems, Man and Cybernetics, Part C: Applications and Reviews, Vol. 42, No. 6, Nov. 2012, pp. 1613 – 1623.

[13] S.R. Velazquez, T.Q. Nguyen, S.R. Broadstone: Design of Hybrid Filter Banks for Analog/Digital Conversion, IEEE Transaction on Signal Processing, Vol. 46, No. 4, Apr. 1998, pp. 956 – 967.

[14] B. Rumberg, D.W. Graham: A Low-power and High-precision Programmable Analog Filter Bank, IEEE Transactions on Circuits and Systems II: Express Briefs, Vol. 59, No. 4, Apr. 2012, pp. 234 – 238.

[15] A. Kammoun, C. Lelandais-Perrault, M. Debbah: SNR Efficient Approach for the Design of Hybrid Filter Bank A/D Converters, IEEE International Conference on Acoustics, Speech and Signal Processing, Vancouver, Canada, 26 – 31 May 2013, pp. 2716 – 2720.

[16] I.W. Selesnick: Lowpass Filters Realizable as Allpass Sums: Design Via a New Flat Delay Filter, IEEE Transaction on Circuits and Systems II: Analog and Digital Signal Processing, Vol. 46, No. 1, Jan. 1999, pp. 40 – 50.

[17] S. Damjanovic, Lj. Milic: A Family of IIR Two-band Orthonormal QMF Filter Banks, Serbian Journal of Electrical Engineering, Vol. 1, No. 3, Sept. 2004, pp. 45 – 56.

[18] J.H. Lee, Y.H. Yang: Optimal Design of Complex Two-channel IIR QMF Banks with Equiripple Response, IEICE Transactions on Fundamentals of Electronics, Communications and Computer Science, Vol. E88-A, No. 8, Aug. 2005, pp. 2143 – 2153.

[19] S. Koshita, M. Abe, M. Kawamata: State-space Analysis of Power Complementary Analog Filters, IEEE International Symposium on Circuits and Systems, New Orleans, LA, USA, 27 – 30 May 2007, pp. 2814 – 2817.
[20] J.H. Lee, Y.H. Yang: Design of Two-channel Linear-phase QMF Banks based on Real IIR All-pass Filters, IEE Proceedings - Vision, Image and Signal Processing, Vol. 150, No. 5, Oct. 2003, pp. 331 – 338.
[21] G.C. Temes, J.W. LaPatra: Introduction to Circuits Synthesys and Design, McGraw Hill, NY, USA, 1977.
[22] M.D. Lutovac, D.V. Tosic, B.L. Evans: Filter Design for Signal Processing using Matlab and Matematica, Prentice Hall, NJ, USA, 2001.
[23] P.P. Vaidyanathan: Some Properties of IIR Power-symmetric Filters, IEEE International Conference on Acoustics, Speech and Signal Processing, Honolulu, HI, USA, 15 – 20 Apr. 2007, Vol. 3, pp. III 1449 – III 1452.
[24] D. Zivaljevic, V. Stojanovic: Transitional Butter-elliptic Filter Suitable for Complementary Decomposition, Inverse Problems in Science and Engineering, Vol. 20, No. 1, Jan. 2012, pp. 117 – 125.
[25] H. Zhang, Y. Shi, Z. Wang: A Simple Method to Design Hybrid Analog/Digital Filter Banks Satisfying Near-perfect Reconstruction, International Conference on Communications, Circuits and Systems, Guilin, China, 25 – 28 June 2006, Vol. 4, pp. 2244 – 2247.
[26] H. Lollmann, P. Vary: Design of IIR QMF Banks with Near-perfect Reconstruction and Low Complexity, IEEE International Conference on Acoustics, Speech and Signal Processing, Las Vegas, NV, USA, 31 March – 04 April 2008, pp. 3521 – 3524.
[27] D. Albuquerque, J.M.N. Vieira, N. Carvalho, J. Pereira: Analog Filter Bank for Cochlear Radio, IEEE International Microwave Workshop Series on RF Front-ends for Software Defined and Cognitive Radio Solutions, Aveiro, Portugal, 22 – 23 Feb. 2010, pp. 1 – 4.
[28] C. Grosan, A. Abraham: A New Approach for Solving Nonlinear Equations Systems, IEEE Transactions on Systems, Man and Cybernetics, Part A: Systems and Humans, Vol. 38, No. 3, May 2008, pp. 698 – 714.
[29] W.Y. Yang, W. Cao, T.S. Chung, J. Morris: Applied Numerical Methods using Matlab, John Wiley and Sons, Hoboken, NJ, USA, 2005.
[30] J. Karki: Active Low-pass Filter Design, Texas Instruments, Application Report SLOA049B, Sept. 2002.
[31] A. Williams, F. Taylor: Electronic Filter Design Handbook, McGraw-Hill, NY, USA, 2006.
[32] R.L. Geiger, E. Sanchez-Sinencio: Active Filter Design using Operational Transconductance Amplifiers: A Tutorial, IEEE Circuits and Devices Magazine, Vol. 1, No. 2, March 1985, pp. 20 – 32.
[33] S. Sharma, S. Rana, K. Pal: Realisation of the High Q Notch/Alpass Filter using Low-voltage Current Conveyors, Indian Journal of Pure and Applied Physics, Vol. 48, June 2010, pp. 435 – 437.
[34] R.S. Mathad, M.M. Mutsaddi, S.V. Halse: Studies on Active Filters using OTA-C and Other Current Conveyors, International Journal of Advanced Computer and Mathematical Sciences, Vol. 2, No. 3, 2011, pp. 155 – 159.
[35] T. Deliyannis, Y. Sun, J.K. Fidler: Continuous-time Active Filter Design, CRC Press, Boca Raton, FL, USA, 1999.
[36] A. Gomez, R. Sanahuja, L. Balado, J. Figueras: Analog Circuit Test based on a Digital Signature, Design, Automation Test in Europe Conference and Exhibition, Dresden, Germany, 08 – 12 March 2010, pp. 1641 – 1644.
[37] N.J. Fliege: A New Class of Second-order RC-active Filters with Two Operational Amplifiers, Nachrichtentech Zeitung, Vol. 26, No. 4, June 1973, pp. 279 – 282.